

Novel Thieno-imidazole Based Probe for Colorimetric Detection of Hg^{2+} and Fluorescence Turn-on Response of Zn^{2+}

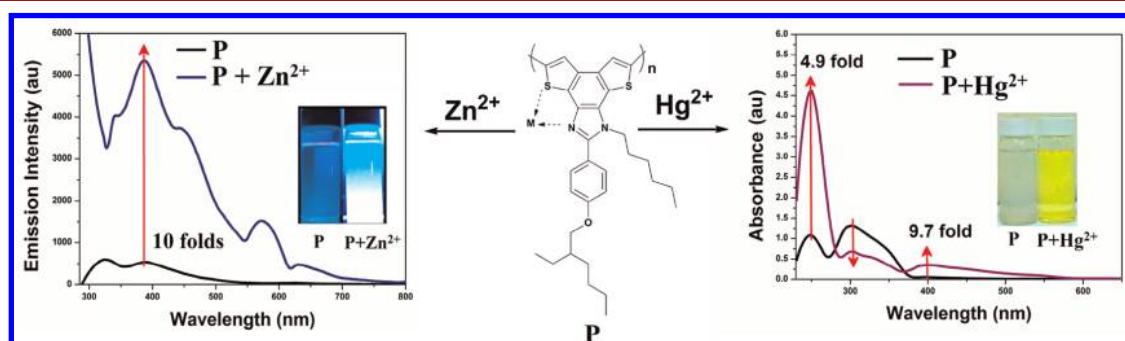
Rudrakanta Satapathy, Yen-Hsing Wu, and Hong-Cheu Lin*

Department of Materials Science and Engineering, National Chiao Tung University, Hsinchu 30049, Taiwan (ROC)

linhc@mail.nctu.edu.tw

Received April 5, 2012

ABSTRACT



Novel thieno-imidazole based polymer P showed both colorimetric and ratiometric detections of Hg^{2+} as well as fluorometric detection of Zn^{2+} via fluorescence turn-on response with augmented lifetime. Its model polymer M did not show any such sensing capability under similar conditions, which further confirmed the unique sensitivity of P toward Hg^{2+} and Zn^{2+} via the chelation of metal ions to both “S” and “N” heteroatoms.

Owing to the ghastly immunotoxic, genotoxic, neurotoxic, malnutrition, and digestive disorder effects, mercury is considered to be a highly dangerous element in the environment, which can be easily bioaccumulated.¹ Zinc, a pervasive second most essential transition element in the human body after iron, is involved in numerous biological processes, such as cellular metabolism, neurotransmission, signal transduction, gene expression, apoptosis, as well as pathological processes in many diseases (including Alzheimer’s disease, epilepsy, ischemic stroke, and so forth).² It is thus imperative to develop analytic and detective methods for sensitive sensing of Zn^{2+} and Hg^{2+} . Unlike other biological transition metal ions, such as Fe^{2+} , Mn^{2+} , and Cu^{2+} ions, both Zn^{2+} and Hg^{2+} ions are spectroscopically

and magnetically neutral and thus do not give any signals due to their $3d^{10}4s^0$ (Zn^{2+}) and $5d^{10}6s^0$ (Hg^{2+}) electronic configurations. Thus common analytic techniques, such as Mossbauer, nuclear magnetic resonance (NMR), and electron paramagnetic resonance (EPR), are unable to detect this archetypal metal ion in biological systems. Furthermore, fluorescence offers significant advantages over other methods for detection of these metal ions because of

(1) (a) Zhang, Z.; Wu, D.; Guo, X.; Qian, X.; Lu, Z.; Xu, Q.; Yang, Y.; Duan, L.; He, Y.; Feng, Z. *Chem. Res. Toxicol.* **2005**, *18*, 1814. (b) Harada, M. *Crit. Rev. Toxicol.* **1995**, *25*, 1. (c) Renzoni, A.; Zino, F.; Franchi, E. *Environ. Res.* **1998**, *77*, 68. (d) Benoit, J. M.; Fitzgerald, W. F.; Damman, A. W. *Environ. Res.* **1998**, *78*, 118.

(2) (a) Que, E. L.; Domaille, D. W.; Chang, C. J. *Chem. Rev.* **2008**, *108*, 1517 and references therein. (b) Frederickson, C. J.; Koh, J. Y.; Bush, A. I. *Nat. Rev. Neurosci.* **2005**, *6*, 449. (c) Scrimgeour, A. G.; Stahl, C. H.; McClung, J. P.; Marchitelli, L. J.; Young, A. J. *J. Nutri. Biol.* **2007**, *18*, 813.

(3) (a) Amendola, V.; Fabbrizzi, L.; Forti, F.; Licchelli, M.; Mangano, C.; Pallavicini, P.; Poggi, A.; Sacchi, D.; Taglietti, A. *Coord. Chem. Rev.* **2006**, *250*, 273. (b) Rurack, K.; Resch-Genger, U. *Chem. Soc. Rev.* **2002**, *31*, 116. (c) Valeur, B.; Leray, I. *Coord. Chem. Rev.* **2000**, *205*, 3. (d) Yoon, J.; Kim, S. K.; Singh, N. J.; Kim, K. S. *Chem. Soc. Rev.* **2006**, *35*, 355. (e) Mutihac, L.; Lee, J. H.; Kim, J. S.; Vicens, J. *Chem. Soc. Rev.* **2011**, *40*, 2777. (f) Xu, Z.; Singh, N. J.; Lim, J.; Pan, J.; Kim, H. N.; Park, S. S.; Kim, K. S.; Yoon, J. *J. Am. Chem. Soc.* **2009**, *131*, 15528.

(4) (a) Que, E. L.; Domaille, D. W.; Chang, C. J. *Chem. Rev.* **2008**, *108*, 1517. (b) Jiang, P.; Guo, Z. *Coord. Chem. Rev.* **2004**, *248*, 205. (c) Xu, Z.; Yoon, J.; Spring, D. R. *Chem. Soc. Rev.* **2010**, *39*, 1996. (d) Burdette, S. C.; Frederickson, C. J.; Bu, W.; Lippard, S. J. *J. Am. Chem. Soc.* **2003**, *125*, 1778. (e) Brombosz, S. M.; Zuccherro, A. J.; Phillips, R. L.; Vazquez, D.; Wilson, A.; Bunz, U. H. F. *Org. Lett.* **2007**, *9*, 4519. (f) Wong, K. M. C.; Tang, W. S.; Lu, X. X.; Zhu, N.; Yam, V. W. *Inorg. Chem.* **2005**, *44*, 1492. (g) Peng, X.; Xu, Y.; Sun, S.; Wu, Y.; Fan, J. *Org. Biomol. Chem.* **2007**, *5*, 226. (h) Quang, D. T.; Kim, J. S. *Chem. Rev.* **2007**, *107*, 3780. (i) Chen, W. H.; Xing, Y.; Pang, Y. *Org. Lett.* **2011**, *13*, 1362.

simplicity, nondestructive character, high sensitivity, and instantaneous response.³ Consequently, noninvasive fluorescence technique is a mode of choice for metal ion imaging.⁴

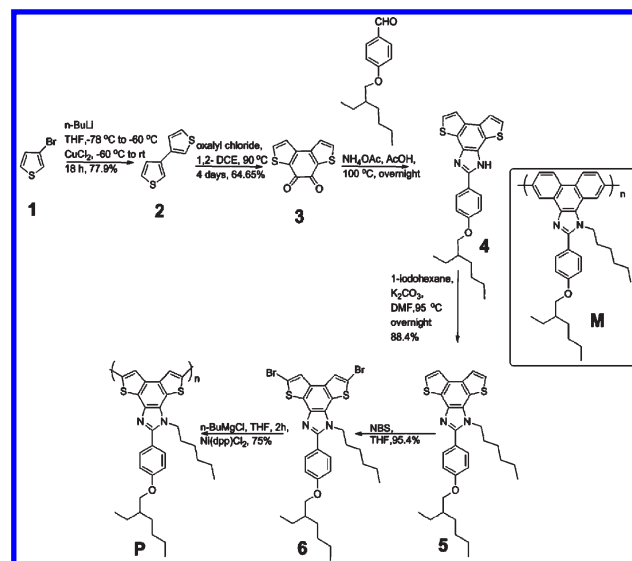
The furthest advantage of fluorescence “turn-on” sensors related to “turn-off” sensors is the ease of detecting low-concentration contrast relative to a “dark” background, which reduces the possibility of false positive signals and enhances the sensitivity, as demonstrated by numerous studies.⁵ The intramolecular charge transfer (ICT)-based fluorescence mechanism has been widely used to illustrate fluorescence turn-on and turn-off behaviors for various sensory materials.⁶ Furthermore, ratiometric fluorescent probes have immense significance because they permit signal ratio corresponding to more than one wavelength and provide built-in correction for environmental effects.⁷ The naked eye perceived color change would be beneficial for instantaneous visual sensing.

Numerous probes have been reported for sensing of Hg^{2+} , for example, bis(*N*-methylindolyl)methane,^{8a} amino acid,^{8b,c} indole,^{8d} sulfonamide,^{8e} triazole-based dansyl,^{8f} methionine,^{8g} and rhodamine.^{8h} Likewise several probes have been designed for Zn^{2+} sensing, such as dipicolylamine,^{9a,b} DPA,^{9c} TPEN,^{9d} and Schiff base derivatives.^{9e} Since the sulfur atom is considered to be a “soft” donor atom, it can act as a chelating agent and also increase the sensor’s affinity and selectivity for binding transition metal cations.

Herein, we synthesized thieno-imidazole based polymer **P** (Scheme 1), with neighboring nitrogen and sulfur heteroatoms as chelating sites for metal ions. This was found to be a suitable design for colorimetric detection of Hg^{2+} and fluorometric detection of Zn^{2+} . 3,3'-Bithiophene was prepared from 3-bromothiophene by treating with *n*-BuLi and CuCl_2 , which was further acylated without any Lewis acid to produce compound **3**. Then, it was coupled with 4-((2-ethylhexyl)oxy)benzaldehyde by refluxing in the presence of acetic acid and NH_4OAc to obtain compound **4**. *N*-Alkylation of **4** by hexyliodide and K_2CO_3 yielded compound **5**, which was brominated by NBS to obtain monomer **6**. Finally, Grignard polymerization of monomer **6** by CH_3MgBr and NiDPPCl_2 produced polymer **P**. To compare the selectivity of polymer **P** toward metal ions,

model polymer **M** (where only a single nitrogen atom in the imidazole ring is available for binding) was synthesized. Synthesis of model polymer **M** is depicted in Supplementary Scheme S1.

Scheme 1. Synthesis of Polymer **P**



To verify the sensing abilities of metal ions, polymer **P** was titrated over a wide range of metal ions, such as Na^+ , K^+ , Ba^{2+} , Ca^{2+} , Ni^{2+} , Cu^+ , Co^{2+} , Ag^+ , Zn^{2+} , and Hg^{2+} (Supplementary Figure S1). Originally, two absorption maxima at 248 and 303 nm appeared in polymer **P**. Upon the sequential addition of Hg^{2+} , a significant change in absorption pattern was observed. As shown in Figure 1a, the final intensities of the peak at 248 nm increased ca. 4.9-fold, and the peak at 303 nm decreased ca. 50%. Furthermore, a new peak appeared at 395 nm and increased almost 9.7-fold. Two clear isosbestic points at 281 and 367 nm were obtained upon titration with Hg^{2+} . The intensities at 305 and 248 nm (Figure 1b) as well as 395 and 305 nm (Figure 1c) were compared, which showed the intensity changed almost linearly with the concentration of Hg^{2+} . The color of the polymer solution changed from colorless to yellow, which could be easily detected by the naked eye. However, other metal ions did not show such alteration in absorption pattern. A Job plot was plotted to find the stoichiometry during the binding of Hg^{2+} (Supplementary Figure S2). The variation of absorption intensities at 385 and 305 nm ($A_{385} - A_{305}$) as a function of molar ratio $X_M = [\text{Hg}^{2+}]/([\text{Hg}^{2+}] + [\text{P}])$ showed 1:1 stoichiometry. ^1H NMR titration was further conducted to elucidate the binding mode, and the NMR titration spectra of monomer **6** (in *d*-THF) upon the addition of 0–1.1 equiv of Hg^{2+} (in D_2O) are depicted in Figure 2. Notable downfield shifts of peaks corresponding to the aromatic protons of monomer **6** were observed upon the gradual addition of Hg^{2+} . However, no further changes in ^1H NMR signals were observed at higher equivalents of Hg^{2+} . This result is consistent with 1:1 binding stoichiometry of Hg^{2+} with

(5) (a) Rurack, K.; Kollmannsberger, M.; Resch-Genger, U.; Daub, J. *J. Am. Chem. Soc.* **2000**, *122*, 968. (b) McQuade, D. T.; Hegedus, A. H.; Swager, T. M. *J. Am. Chem. Soc.* **2000**, *122*, 12389.

(6) (a) Kim, J. S.; Quang, D. T. *Chem. Rev.* **2007**, *107*, 3780. (b) Zhang, J. F.; Lim, C. S.; Bhuniya, S.; Cho, B. R.; Kim, J. S. *Org. Lett.* **2011**, *13*, 1190.

(7) Yuan, L.; Lin, W.; Chen, B.; Xie, Y. *Org. Lett.* **2012**, *14*, 432.

(8) (a) Kaur, P.; Kaur, S.; Singh, K. *Org. Biomol. Chem.* **2012**, *10*, 1497. (b) Yang, M. H.; Thirupathi, P.; Lee, K. H. *Org. Lett.* **2011**, *13*, 5028. (c) Lohani, C. R.; Kim, J. M.; Lee, K. H. *Tetrahedron* **2011**, *67*, 4130. (d) Kaur, P.; Kaur, S.; Singh, K.; Sharma, P. R.; Kaur, T. *Dalton Trans.* **2011**, *40*, 10818. (e) Joshi, B. P.; Lohani, C. R.; Lee, K. H. *Org. Biomol. Chem.* **2010**, *8*, 3220. (f) Neupane, L. N.; Kim, J. M.; Lohani, C. R.; Lee, K. H. *J. Mater. Chem.* **2012**, *22*, 4003. (g) Yang, M. H.; Lohani, C. R.; Cho, H.; Lee, K. H. *Org. Biomol. Chem.* **2011**, *9*, 2350. (h) Kumar, M.; Kumar, N.; Bhalla, V.; Singh, H.; Sharma, P. R.; Kaur, T. *Org. Lett.* **2011**, *13*, 1422.

(9) (a) Zhang, J. F.; Kim, S.; Han, J. H.; Lee, S. J.; Pradhan, T.; Cao, Q. Y.; Lee, S. J.; Kang, C.; Kim, J. S. *Org. Lett.* **2011**, *13*, 5294. (b) Xu, Y.; Pang, Y. *Dalton Trans.* **2011**, *40*, 1503. (c) Xu, Y.; Pang, Y. *J. Chem. Commun.* **2010**, *46*, 4070. (d) Hanaoka, K.; Muramatsu, Y.; Urano, Y.; Terai, T.; Nagano, T. *Chem.—Eur. J.* **2010**, *16*, 568. (e) Wang, L.; Qin, W.; Tang, X.; Dou, W.; Liu, W. *J. Phys. Chem. A* **2011**, *115*, 1609.

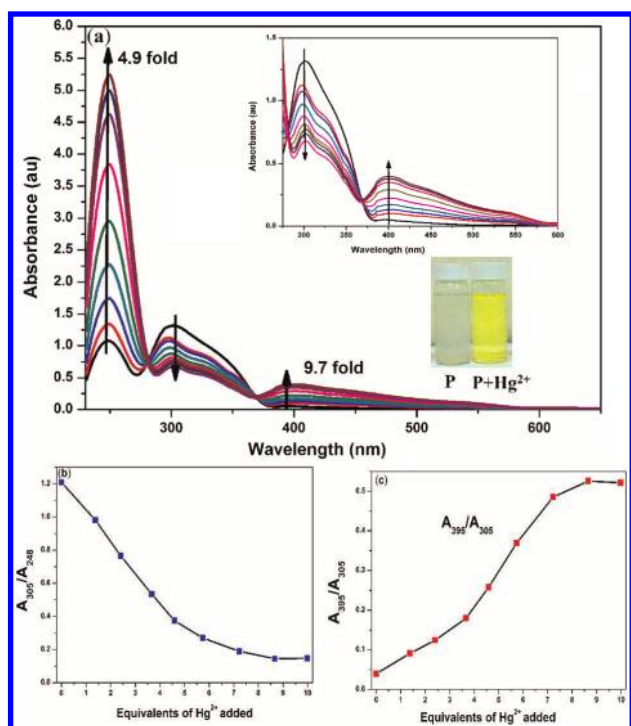


Figure 1. (a) Absorption spectral changes of **P** (1.1×10^{-5} M) in THF/H₂O (1:1) upon titration with (0– 1.1×10^{-4} M) of Hg²⁺. Upper inset: absorption pattern from 275 to 600 nm. Lower inset: color change upon the addition of Hg²⁺. Absorption spectral ratios (b) A_{305}/A_{248} and (c) A_{395}/A_{205} as a function of equivalents of Hg²⁺ added.

polymer **P**. This result is consistent with 1:1 binding stoichiometry of Hg²⁺ with polymer **P**. The binding constant for binding of Hg²⁺ was calculated to be 0.74×10^5 from Supplementary Figure S3.

Model polymer **M** (where the binding site is only nitrogen heteroatom in the imidazole ring) showed two absorption maxima at 267 and 290 nm. Polymer **M** was titrated with Hg²⁺ under the similar condition as that of polymer **P**. However, unlike polymer **P**, no additional peak appeared and the absorption pattern was not changed substantially (Supplementary Figure S4). This may be attributed to the susceptibility of Hg²⁺ to be bound between “S” and “N” of thio-imidazole unit in polymer **P**. Thus, it is concluded that the thio-imidazole based probe is a suitable design for the colorimetric detection of Hg²⁺.

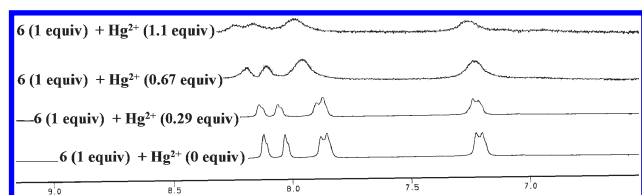


Figure 2. ¹H NMR spectra (aromatic region) of monomer **6** upon the addition of 0–1.1 equiv of Hg²⁺ wrt [**6**].

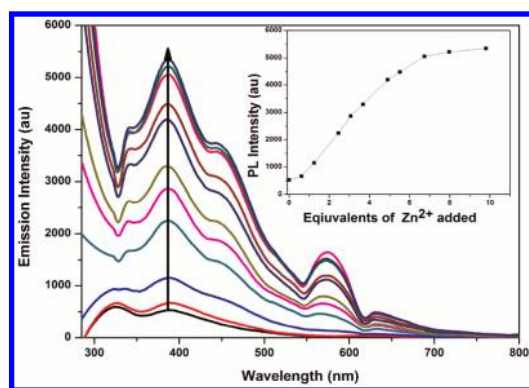


Figure 3. Fluorescence spectral response of **P** (1.1×10^{-5} M) in THF/H₂O (1/1) acquired by the sequential addition of 0–10 equiv of Zn²⁺. Inset: Intensity of **P** as a function of equiv of Zn²⁺ added.

Similarly, the fluorescence patterns of polymer **P** upon the addition of various metal ions under similar conditions are depicted in Supplementary Figure S5, and their histograms are shown in Supplementary Figure S6. As observed in Figure 3, upon the addition of Zn²⁺, the fluorescence intensity increased ca. 10-fold, which was the most significant change in fluorescence signals compared with the other metal ions. The lone-pair electrons in the thio-imidazole receptor undergo rapid electron transfer, which causes the weak fluorescence of **P**. In the presence of suitable cationic analytes (here Zn²⁺), the nonbonding electrons get coordinated and thus the ICT effect is inhibited, which resulted in the strong fluorescence of **P**. Thus, in the presence of Zn²⁺, **P** showed a remarkable increase in the intensity of the emission band with a chelation enhanced fluorescence factor (CHEF)¹⁰ = 10.5. Again, it resulted in a 14.3-fold enhancement of the quantum yield for polymer **P** (from $\Phi = 0.03$ to $\Phi = 0.43$). From the fluorescence binding isotherm, the association constant was calculated to be $K_a = 5.14 \times 10^6$ M⁻¹. To find the interference of other background cations, we conducted the titrations by using a dual metal system (Supplementary Figure S7). The enhanced fluorescence of polymer **P** in the presence of Zn²⁺ was not substantially perturbed by the background cations. To gain insight into the binding of Zn²⁺ with the repeating unit of **P**, ¹H NMR titration was carried out by the gradual addition of Zn²⁺ (in D₂O) to monomer **6** (in *d*-THF). As shown in Figure 4, a momentous upfield shift of peaks corresponding to the aromatic protons of monomer **6** was observed upon the sequential addition of Hg²⁺ (0–1.1 equiv). Fluorometric titration of Zn²⁺ was conducted for model polymer **M** to investigate the effect of Zn²⁺. Model polymer **M** did not show any significant fluorescence enhancement in the presence of Zn²⁺ under similar conditions (see Supplementary Figure S8). As shown in Table 1, the quantum yield of **M** revealed only a 2.25-fold increase (from $\Phi = 0.04$ to $\Phi = 0.09$), and

(10) Satapathy, R.; Wu, Y. H.; Lin, H. C. *Chem. Commun.* **2012**, DOI: 10.1039/C2CC31131C.

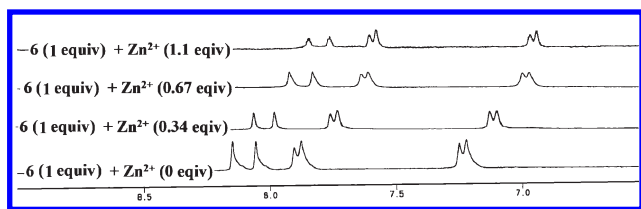


Figure 4. ^1H NMR spectra (aromatic region) of monomer **6** upon the addition of 0–1.1 equiv of Zn^{2+} wrt [**6**].

correspondingly the CHEF was increased just up to 2.2 times. Furthermore, the association constant of polymer **P** with Zn^{2+} was calculated as 5.14×10^6 , which is almost 3.8×10^3 times higher than that of polymer **M**. To elucidate the effect of polymerization, we further carried out the fluorescence titration of compound **5** with Zn^{2+} . Upon the addition of equivalent amounts of Zn^{2+} , the fluorescence intensities of compound **5** were sequentially increased merely up to 4 times (Supplementary Figure S9). Thus, in contrast to the small molecular analogue **5** (CHEF = 3.8), the increased sensitivity of polymer **P** (CHEF = 10.5) is due to the molecular ion effect with a larger number of binding sites in polymer **P**.

Time-resolved fluorescence measurements¹⁰ were performed for both polymer **P** and its Zn^{2+} -complex probed at 390 nm (excited at 375 nm), as shown in Figure 5. In the absence of Zn^{2+} , a single exponential fitting for the fluorescence lifetime of polymer **P** was estimated as 0.49 ns, which corresponded to the lifetime of the S1 state. Upon the addition of Zn^{2+} , the fluorescence lifetime corresponding to the S1 state was elevated to 2.96 ns. No remarkable change in fluorescence lifetime of model polymer **M** was observed under similar conditions (see Table 1 and Supplementary Figure S10).

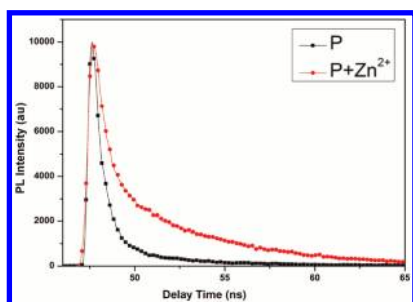


Figure 5. Time-resolved fluorescence spectral responses for polymer **P** before and after the addition of Zn^{2+} .

Upon the progressive addition of Zn^{2+} , two oxidation peaks Ox_1 and Ox_2 of polymer **P** were anodically shifted and disappeared, respectively (see Supplementary Figure S11), and the half-wave oxidation potential ($E_{1/2}$) of Ox_1 (appeared at 1520 mV originally) was shifted to 1200 mV with $\Delta E_{1/2} = 320$ mV. This indicated a less favorable

Table 1. Quantum Yields, Fluorescence Lifetimes, Association Constants, and CHEF Values of Polymers **P** and **M** upon the Addition of Zn^{2+}

	Φ^a	lifetime ^b	K_a^c	CHEF ^d
P	0.03	0.49	NA	NA
P + Zn^{2+}	0.43	2.96	5.14×10^6	10.5
M	0.04	0.34	NA	NA
M + Zn^{2+}	0.09	0.37	1.35×10^3	2.26

^aQuantum yields calculated using tryptophan (in H_2O) as a standard. ^bObtained from time-resolved fluorescence measurements. ^cAssociation constants calculated from the slopes of binding isotherms. ^dCHEF is defined as I/I_0 , where I is the maximum emission intensity of the receptor–metal complex and I_0 is the maximum emission intensity of the free receptor.

oxidation process for polymer **P** due to the presence of close proximity of a positively charged Zn cation center. Furthermore, the HOMO level of polymer **P** was lowered (from -5.36 to -5.56), and its LUMO level was increased (from -3.92 to -3.42) after complexation with Zn^{2+} . Thus, the obstruction of the reductive as well as oxidative ICT caused the enhancement of the fluorescent intensity.

To check the affinities of different anions toward a **P**-Zn complex, we added various anions, such as F^- , Cl^- , Br^- , I^- , S^{2-} , NO_3^- , Ac^- , PO_4^{3-} , and SCN^- , to the solution of **P**-Zn complex. Surprisingly, unlike other anions, upon the addition of I^- , the color of the solution changed from colorless to yellow (Supplementary Figure S12a). The progressive appearance of a new peak at 375 nm was observed upon the sequential addition of I^- (Supplementary Figure S12b). Thus, **P**-Zn complex is susceptible for the colorimetric detection of I^- ions. Reversible association of Zn^{2+} with polymer **P** was achieved by the addition of $\text{Na}_2\text{-EDTA}$ as a suitable counter ligand (Supplementary Figure S13). Therefore, the on–off–on fluorescence etiquette was successfully achieved via the alternate addition of Zn^{2+} and $\text{Na}_2\text{-EDTA}$ for 5 successive cycles (Supplementary Figure S14).

In summary, the naked-eye detection of Hg^{2+} was achieved by polymer **P** with a thieno-imidazole backbone. Furthermore, polymer **P** showed a fluorescence turn-on response with an enhanced fluorescence lifetime in the presence of Zn^{2+} . Its model polymer **M** could not show any such remarkable sensitivity toward Hg^{2+} and Zn^{2+} , which confirmed the unique sensitivity of **P** via the chelation of metal ions to both “S” and “N” heteroatoms. Moreover, the colorimetric detection of I^- was selectively accomplished by **P**-Zn complex over other anions.

Acknowledgment. Financial support of this project was provided by the National Science Council of Taiwan (ROC) through NSC 99-2113-M-009-006-MY2.

Supporting Information Available. Synthetic procedures, Figures S1–S12, and NMR spectral data. This material is available free of charge via the Internet at <http://pubs.acs.org>.

The authors declare no competing financial interest.